RESEARCH ARTICLE

JBMR®

Al-Gazali Skeletal Dysplasia Constitutes the Lethal End of *ADAMTSL2*-Related Disorders

Dominyka Batkovskyte,[1] Fiona McKenzie,[2,3] Fulya Taylan,[1,4] Pelin Ozlem Simsek-Kiper,[5] Sarah M Nikkel,[6,7] Hirofumi Ohashi,[8] Roger E Stevenson,[9] Thuong Ha,[10,11,12] Denise P Cavalcanti,[13] Hiroyuki Miyahara,[14] Steven A Skinner,[9] Miguel A Aguirre,[15] Zühal Akçören,[16] Gulen Eda Utine,[5] Tillie Chiu,[17] Kenji Shimizu,[8] Anna Hammarsjö,[1,4] Koray Boduroglu,[5] Hannah W Moore,[9] Raymond J Louie,[9] Peer Arts,[10,12] Allie N Merrihew,[9] Milena Babic,[10,18] Matilda R Jackson,[10,18,19] Nikos Papadogiannakis,[20] Anna Lindstrand,[1,4] Ann Nordgren,[1,4,21,22] Christopher P Barnett,[23,24] Hamish S Scott,[10,11,12,18,24] Andrei S Chagin,[25,26] Gen Nishimura,[1,27] and Giedre Grigelioniene[1,4]

[1]Department of Molecular Medicine and Surgery and Center for Molecular Medicine, Karolinska Institutet, Stockholm, Sweden
[2]Genetic Services of Western Australia, Perth, Australia
[3]School of Pediatrics and Child Health, University of Western Australia, Perth, Australia
[4]Department of Clinical Genetics, Karolinska University Hospital, Stockholm, Sweden
[5]Division of Pediatric Genetics, Department of Pediatrics, Faculty of Medicine, Hacettepe University, Ankara, Turkey
[6]Provincial Medical Genetics Program, BC Women's Hospital, Vancouver, Canada
[7]University of British Columbia, Vancouver, Canada
[8]Division of Medical Genetics, Saitama Children's Medical Center, Saitama, Japan
[9]Greenwood Genetic Center, Greenwood, SC, USA
[10]Genetics and Molecular Pathology Research Laboratory, Centre for Cancer Biology, An Alliance between SA Pathology and the University of South Australia, Adelaide, Australia
[11]ACRF Cancer Genomics Facility, Centre for Cancer Biology, An Alliance between SA Pathology and the University of South Australia, Adelaide, Australia
[12]UniSA Clinical and Health Sciences, University of South Australia, Adelaide, Australia
[13]Skeletal Dysplasias Group, Department of Translational Medicine, Medical Genetics, University of Campinas (UNICAMP), Campinas, Brazil
[14]Division of Neonatology, Kawaguchi City Medical Center, Kawaguchi, Japan
[15]Centro Nacional de Genética Médica (CENAGEM), A.N.L.I.S "Dr. Carlos G. Malbrán", Buenos Aires, Argentina
[16]Division of Pediatric Pathology, Department of Pediatrics, Faculty of Medicine, Hacettepe University, Ankara, Turkey
[17]CHEO Genetics Clinic, Regional Genetics Program, Ottawa, Canada
[18]Department of Genetics and Molecular Pathology, SA Pathology, Adelaide, Australia
[19]Australian Genomics Health Alliance, Melbourne, Australia
[20]Department of Laboratory Medicine, Division of Pathology, Karolinska Institutet, Department of Pathology, Karolinska University Hospital, Stockholm, Sweden
[21]Department of Clinical Genetics and Genomics, Sahlgrenska University Hospital, Gothenburg, Sweden
[22]Institute of Biomedicine, Department of Laboratory Medicine, University of Gothenburg, Gothenburg, Sweden
[23]Pediatric and Reproductive Genetics Unit, South Australian Clinical Genetics Service, Women's and Children's Hospital, North Adelaide, Australia
[24]Adelaide Medical School of Medicine, University of Adelaide, Adelaide, Australia
[25]Department of Physiology and Pharmacology, Karolinska Institutet, Stockholm, Sweden
[26]Institute of Medicine, Gothenburg University, Gothenburg, Sweden
[27]Department of Radiology, Musashino-Yowakai Hospital, Tokyo, Japan

Received in original form November 25, 2022; revised form March 1, 2023; accepted March 4, 2023.
Address correspondence to: Giedre Grigelioniene, MD, PhD, Department of Molecular Medicine and Surgery, Karolinska Institutet, Visionsgatan 4, 17164 Solna, Stockholm, Sweden. E-mail: giedre.grigelioniene@ki.se
Additional Supporting Information may be found in the online version of this article.

Journal of Bone and Mineral Research, Vol. 38, No. 5, May 2023, pp 692–706.

DOI: 10.1002/jbmr.4799

ABSTRACT

Lethal short-limb skeletal dysplasia Al-Gazali type (OMIM %601356), also called dysplastic cortical hyperostosis, Al-Gazali type, is an ultra-rare disorder previously reported in only three unrelated individuals. The genetic etiology for Al-Gazali skeletal dysplasia has up until now been unknown. Through international collaborative efforts involving seven clinical centers worldwide, a cohort of nine patients with clinical and radiographic features consistent with short-limb skeletal dysplasia Al-Gazali type was collected. The affected individuals presented with moderate intrauterine growth restriction, relative macrocephaly, hypertrichosis, large anterior fontanelle, short neck, short and stiff limbs with small hands and feet, severe brachydactyly, and generalized bone sclerosis with mild platyspondyly. Biallelic disease-causing variants in *ADAMTSL2* were detected using massively parallel sequencing (MPS) and Sanger sequencing techniques. Six individuals were compound heterozygous and one individual was homozygous for pathogenic variants in *ADAMTSL2*. In one of the families, pathogenic variants were detected in parental samples only. Overall, this study sheds light on the genetic cause of Al-Gazali skeletal dysplasia and identifies it as a semi-lethal part of the spectrum of *ADAMTSL2*-related disorders. Furthermore, we highlight the importance of meticulous analysis of the pseudogene region of *ADAMTSL2* where disease-causing variants might be located. © 2023 The Authors. *Journal of Bone and Mineral Research* published by Wiley Periodicals LLC on behalf of American Society for Bone and Mineral Research (ASBMR).

KEY WORDS: SKELETAL DYSPLASIA; ADAMTSL2; NEONATAL LETHAL; GELEOPHYSIC DYSPLASIA; AL-GAZALI SKELETAL DYSPLASIA; BONE SCLEROSIS

Introduction

Short-limb skeletal dysplasia Al-Gazali is a rare neonatal lethal skeletal dysplasia, which has previously only been described in three unrelated individuals.[1,2] The main skeletal features are severe growth retardation, short limbs, generally sclerotic bones, broad and underdeveloped ribs and clavicles, short long bones, mild platyspondyly, and severe brachydactyly. Craniofacial morphology includes relatively large head with a wide anterior fontanelle, flat facial profile, low-set ears, short nose, and thin lips.[1,2] Other characteristics are hypertrichosis, mildly hypoplastic thorax, and joint stiffness. Radiological characteristics include increased bone density, short tubular bones, wide diaphyses, and round metaphyses. In the previously reported individuals, no genetic etiology was identified. Phenotypically similar but milder skeletal dysplasia caused by biallelic variants in *ADAMTSL2* is geleophysic dysplasia type 1 (GPHYSD1, OMIM #231050). Twenty-nine pathogenic variants in the *ADAMTSL2* gene have been reported in 43 individuals with GPHYSD1.[3,4] GPHYSD1 is a rare autosomal recessive disorder generally characterized by severe short stature, small hands and feet, restricted joint movement, joint contractures, distinctive facial features, tip-toe walking, and thickened skin. Skeletal features include broad proximal phalanges, cone-shaped epiphyses, delayed bone age, osteopenia, short tubular bones, and ovoid vertebral bodies.[5,6] In addition, recurrent respiratory infections, tracheal stenosis, and progressive cardiac disease are common and often lead to an early death.[5,7] In the current nosology and classification of genetic skeletal disorders, GPHYSD1 belongs to the group of acromelic dysplasias.[8] Acromelic dysplasias collectively form a group of rare connective tissue disorders that share distinct musculoskeletal features, such as short stature, brachydactyly, joint stiffness, pseudomuscular build, and thick, tight skin.[3] Most of the genes related to acromelic dysplasias encode secreted extracellular matrix (ECM) proteins that are important for microfibrillar network assembly and regulation of TGFβ and BMP signaling pathways.[3]

Human *ADAMTSL2* (NM_014694.4, ENST00000393060.1, hg19) is composed of 19 exons, of which the first is non-coding, and exons 10–19 share sequence homology with a pseudogene region. Low expression of *ADAMTSL2* in commonly clinically available tissues, such as dermal fibroblasts and blood, has been reported in adults (GTEx, https://gtexportal.org/). Expression of *ADAMTSL2* was also shown to be undetectable in cultured human fetal cardiac fibroblasts.[9]

Through international collaboration, a cohort of nine patients with a clinical diagnosis of lethal skeletal dysplasia Al-Gazali type and disease-causing variants in the *ADAMTSL2* gene was collected. We present a summary of clinical, radiological, and genetic data and show that in the less severe cases, survival into early childhood is possible. However, the condition is associated with high perinatal mortality most often caused by respiratory and cardiac failure.

Patients and Methods

Patients and clinical records

Clinicians with patients with clinical diagnosis of Al-Gazali skeletal dysplasia were invited to recruit the families to this study. All referring physicians are members of the International Skeletal Dysplasia Network that facilitated this collaboration. Nine affected individuals from seven non-consanguineous and one consanguineous family were included in this study. Clinical findings of patient 1 from a Swedish family and patient 2 from a Japanese family were described previously.[2] In family 3, two fetuses were clinically diagnosed with Al-Gazali skeletal dysplasia, but DNA sample was available only from one fetus. Clinical data were collected from patient records by their referring physicians. Genomic DNA was extracted from blood, frozen fetal tissues, or primary cells as summarized in Supplemental Table S1. DNA from the first patient identified with Al-Gazali skeletal dysplasia was not available (personal communication with Prof L Al-Gazali).

Genetic analysis

Different sequencing approaches were performed for each patient in this study as shown in Supplemental Table S1. Initially, testing by exome sequencing was completed on DNA samples from family trios 1, 2, and 3, which led to identification of only two heterozygous a disintegrin and metalloproteinase with thrombospondin motifs-like 2 (*ADAMTSL2*) variants in two of the families. DNA samples from patient 1 and parental samples from family 2 were reanalyzed by whole genome sequencing on Illumina (San Diego, CA, USA) HiSeq X and NovaSeq 600 with median coverage of 30× at Science for Life Laboratory (SciLifeLab, Stockholm, Sweden). The amount of DNA from patient 2 was not sufficient for further genome sequencing analysis. DNA samples from family 4 were analyzed by whole

Fig. 1. Pattern of the clinical features of Al-Gazali skeletal dysplasia patients. Patient numbers according to Table 1 are annotated in black and white. (*A*) Overall appearance: short limbs, short neck, narrow thorax, protuberant abdomen, small hands and feet, and talipes equinovarus (mild in patient 2). (*B*) Typical facial features in patients 1, 5, and 6: round facies, hypertrichosis, periorbital puffiness, and anteverted nares. (*C*) Typical head morphology in patients 1, 2, and 5: brachycephaly, short neck, flat face, micrognathia, and small low-set ears with thick helix. (*D*) Typical hand morphology in patients 1, 5, and 6: trident appearance of the hand and severe brachydactyly. (*E*) Close view of lower extremities in patients 1, 5, and 6: equinovarus deformity and short toes. Clinical photos of patients 1 and 2 in *A* and *C* are reproduced with permission from AJMG part A.

Table 1. Summary of Clinical Findings in Al-Gazali Skeletal Dysplasia Patients

	Original report[1]	Patient 1[2]	Patient 2[2]	Patient 3	Patient 4	Patient 5	Patient 6	Patient 7	Patient 8
Sex	F	F	F	M	M	F	F	M	M
Origin	PAK	SWE	JAP	TUR	CAN	JAP	AUS	ARG	USA
GA, weeks +-days	NA, term	31 + 4	26 + 3	24 + 4	20 + 4	38 + 0	30 + 2	28 + 0	39 + 0
Head circumference, cm (*Z*-score)[14,15]									
At birth	NA	29.5 (−0.16)	22.1 (−1.22)	24.0 (+0.17)	19.1 (−1.00)	36.0 (+1.31)	29.0 (+0.5)	25.0 (−0.89)	32.4 (−2.20)
At follow-up						9 months: 45.0 (+0.87)			2 months: 37.8 (−1.13) 11.5 months: 44.5 (−1.20)
Length, cm (*Z*-score)[14,15]									
At birth	38.0	33.0 (−2.91)	26.8 (−2.25)	NA	22.0 (−2.58)	49.0 (−0.60)	35.0 (−1.38)	32.0 (−1.43)	46.9 (−2.13)
At follow-up						9 months: 55.7 (−5.98)			2 months: 50.9 (−3.76) 11.5 months: 63.5 (−4.70)
Weight, g (*Z*-score)[14,15]									
At birth	NA	1710 (−0.16)	682 (−0.80)	756 (−0.28)	341 (−2.07)	3118 (−0.13)	1240 (−0.40)	1085 (−0.16)	2835 (−1.50)
At follow-up						9 months: 7590 (−0.58)			2 months: 4400 (−1.75) 11.5 months: 6900 (−2.50)
Lethal in neonatal period	+	+	+	TOP	TOP	−	+	+	−
General findings									
Polyhydramnios	+	+	+	+	−	+	+	+	+
Hypertrichosis	NA	+	+	+ (Mild)	−	+	+	+	−
Relative macrocephaly	NA	+	+	+	+	+	+	+	+
Short neck	+	+	+	+	−	+	+	+	+
Short limbs	+	+	+	+	+	+	+	+	+
Small hands and feet	+	+	+	+	+	+	+	+	+
Brachydactyly	+	+	+	+	+	+	+	+	+
Club feet	+	+	−	+	+	+	+	+	−
Stiff joints/fixed flexion	NA	+	+	−	− Plantar flexion of feet	+	+	+	+
Thick and tight skin	NA	+	NA	NA	−	+	NA	+	NA
Hydrops	+	+	+	+	−	−	−	Skin edema	NA
Facial morphology									
Abnormal ears	NA	+	+	Low set	Low set	+	+	+	+

(Continues)

Table 1. Continued

General findings									
Hypertelorism	+	+	+	+	Mild	+	+	+	+
Depressed nasal bridge	+	+	+	+	+	+	+	+	+
Thin upper lip	NA	+	+	+	−	+	+	+	+
Midface hypoplasia	+	+	+	+	−	+	+	+	−
Other findings				Long philtrum, prominent right eye globe					
Internal abnormalities									
Cardiovascular system	NA	−	+ Pulmonary stenosis	+ Pulmonary artery hypoplasia and stenosis, Preductal mild aortic coarctation, Right atrial dilatation	−	+ Aortic stenosis Pulmonary stenosis	+ Pulmonary stenosis	+ Perimembranous VSD	+ Pulmonary stenosis
Lung hypoplasia	NA	+	+	+	−	NA	−	NA	−
Brain abnormalities	NA	−	−	Hydrocephaly, bilateral lateral ventricular dilatation, small and shallow posterior fossa	Agenesis of corpus callosum Absence of the cavum septum pellucidum	−	−	Cerebellar hypoplasia	NA

Abbreviations: F = female; M = male; GA = gestational age; NA = not available; TOP = termination of pregnancy; VSD = ventricular septal defect; + = feature present; − = feature absent.

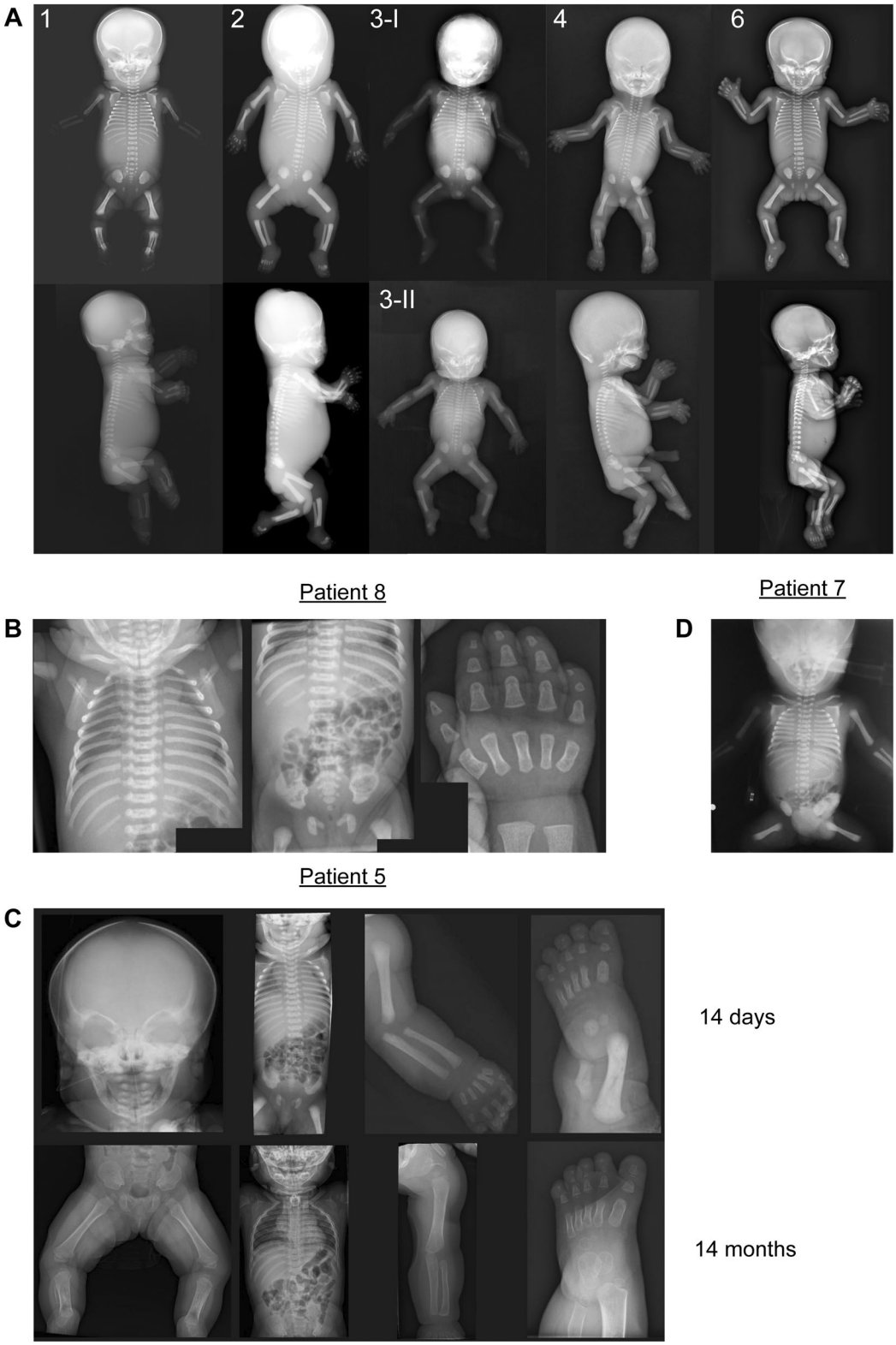

Fig. 2. Radiographic features in Al-Gazali skeletal dysplasia. Patient numbers according to Table 2 are annotated in white. (*A*, *D*) The skeletal phenotypes are homogeneous. The hallmarks include generalized osteosclerosis, large fontanelles, mildly broad ribs, mildly delayed vertebral ossification, delayed ischiopubic ossification, broadening of the long bones, and generalized brachydactyly with a particular shortening of the 1st metacarpal. (*B*) Radiographs of patient 8 at 2 months of age. Note generalized osteosclerosis, broad ribs, delayed ischiopubic ossification, severe brachydactyly, and short first metacarpal. (*C*) Follow-up radiograms of patient 5, who survived up to 14 months, show subsidence of osteosclerosis after birth. Delayed ossification of the vertebral bodies and ischiopubic bones is apparent after birth. Fibular hypoplasia observed in patient 5 is a rare manifestation.

Table 2. Summary of Radiological Signs in Al-Gazali Skeletal Dysplasia Patients

	Original report	Patient 1	Patient 2	Patients 3-I & 3-II	Patient 4	Patient 5	Patient 6	Patient 7	Patient 8
Generalized bone sclerosis	+	+	+	+	+	+	+	+	+
Skull									
Wormian bones	+	−	−	−	−	−	+	NA	−
Wide fontanelles	+	+	+	+	+	+	+	NA	+
Thorax									
Mildly broad ribs	+	+	+	+	+	+	+	+	+
Long bones									
Meta-diaphyseal broadening	+	+	+	+	+	+	+	+	+
Spine									
Mildly delayed vertebral ossification	+	+	+	+	+	+	+	+	+
Pelvis									
Delayed ischiopubic ossification	+	+	+	+	+	+	+	+	+
Hands and feet									
Brachydactyly	+	+	+	+	+	+	+	+	+
Shortening of the 1st metacarpal	+	+	+	+	+	+	+	+	+
Other features					Short fibula	Short, bowed fibula			

Abbreviations: NA = not available; + = feature present; − = feature absent.

genome sequencing on Illumina HiSeq X (SciLifeLab). Bioinformatic analysis and variant calling has been performed as described previously.[10] Variant annotation involves Combined Annotation Dependent Depletion (CADD) score,[11] VEP annotations,[12] and population allele frequencies.[13] Sanger sequencing of the entire *ADAMTSL2* gene was performed on DNA samples from patient 3 and parental samples from family 7 (patient sample was not available for analysis). Illumina DNA PCR-Free Library Prep was used for resequencing the maternal sample from family 7 (Illumina). DNA sample from patient 5 was analyzed by targeted sequencing analysis using TruSight One sequencing panel, including 4813 genes associated with a known clinical phenotype (Illumina). DNA samples from families 6 and 8 were analyzed by whole exome sequencing (WES).

Splice variant analysis

Blood from the father of patient 8 was used to analyze the splice variant. RNA was extracted using PAXgene Blood RNA kit (PreAnalytiX, Hombrechtikon, Switzerland). RNA concentration and quality was determined using Qubit (Thermo Fisher Scientific, Waltham, MA, USA). Synthesis of cDNA was completed using Maxima First Strand cDNA Synthesis Kit (Thermo Fisher Scientific). A semi-nested PCR approach was utilized to increase the DNA amplification for variant analysis.

Cell studies

Dermal fibroblasts were available from patient 1. For controls, two lines of human neonatal dermal fibroblasts (HDFn, source of origin—foreskin) were used, purchased from Thermo Fisher Scientific (cat. no. C-004-5C) and Sigma (St. Louis MO, USA; cat. no. 106-05N). Cells were grown in Dulbecco's Modified Eagle Medium (DMEM) supplemented with high-glucose, GlutaMAX (Thermo Fisher Scientific), 10% fetal bovine serum (FBS) (Thermo Fisher Scientific), 1× non-essential amino acid solution (NEAA) (Thermo Fisher Scientific), and 0.2% primocin (InvivoGen, San Diego, CA, USA). Cells from passages 7–11 were used for experiments.

ADAMTSL2 expression analysis by droplet digital PCR (ddPCR)

RNA from HDFn of patient 1 and controls was extracted using TRIzol reagent (Invitrogen, Waltham, MA, USA) and Direct-zol RNA extraction kit (Zymo Research, Irvine, CA, USA). RNA from the cells was harvested at two time points: 3 to 4 days after seeding, at 95% confluency for the immature extracellular matrix (ECM) conditions, and 7 days after seeding for mature ECM conditions. RNA concentration and quality was determined using Qubit (Thermo Fisher Scientific). Synthesis of cDNA was completed using Maxima First Strand cDNA Synthesis Kit (Thermo Fisher Scientific). Probes against target gene *ADAMTSL2* (FAM labeled) and reference gene *HBB* (HEX labeled) were purchased from Bio-Rad (Hercules, CA, USA) and used with 2X ddPCR Supermix for Probes (No dUTP) according to the manufacturer's recommendations. A maximum of 1300 ng of RNA was used for generating cDNA. Droplets were generated by a QX100 Automated Droplet Generator (Bio-Rad) using DG8 Cartridge (Bio-Rad), and thermal cycling was performed according to the manufacturer's recommendations in C1000 Thermal Cycler (Bio-Rad). The droplets were scanned by QX200 Droplet Reader (Bio-Rad), and the analysis was done using QuantaSoft PRO Analysis Software (Bio-Rad). At least two independent experiments with three biological and three technical replicates were performed.

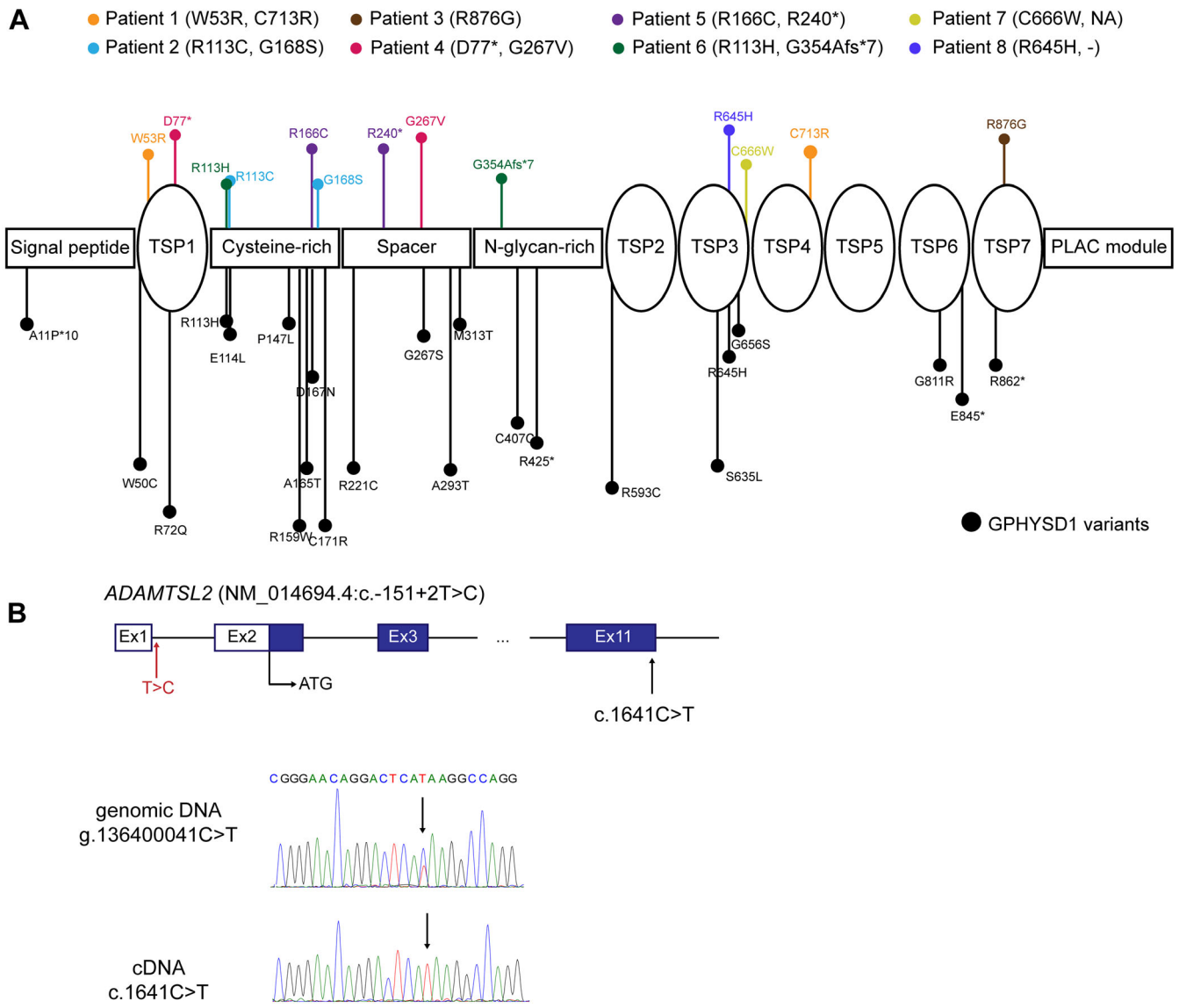

Fig. 3. Genetic findings in Al-Gazali skeletal dysplasia patients. (*A*) Schematic drawing of *ADAMTSL2* protein showing distribution of variants detected in Al-Gazali skeletal dysplasia patients (top, in color) and variants previously reported in geleophysic dysplasia patients (bottom, in black). (*B*) Analysis of *ADAMTSL2* NM_014694.4:c.-151+2T>C splice variant effect in the paternal sample of affected patient 8. Schematic representation of the gene—the nucleotide change is indicated in dark red. Genomic DNA sequence (top) shows the *ADAMTSL2* g.136421044C>T variant in heterozygous state. cDNA sequence (bottom) shows the alternative allele T in hemizygous state (indicated by arrow).

Western blot

Western blot analysis was performed according to standard procedures. Briefly, protein from HDFn of patient 1 and controls was extracted using RIPA lysis buffer (Thermo Fisher Scientific) supplemented with Halt protease and phosphatase inhibitor cocktail (Thermo Fisher Scientific). Protein concentration was measured using Pierce BCA Protein Assay Kit (Thermo Fisher Scientific). An amount of 20 µg protein was used for Western blot. Protein lysates were run on 4% to 15% gradient Mini-PROTEAN TGX precast gels (Bio-Rad) and transferred onto PVDF membrane. Membrane was blocked in 5% BSA for 1 hour at room temperature (RT) after primary antibody incubation at 4°C overnight. Proteins were visualized using Clarity Western ECL substrate (Bio-Rad), and membrane was developed using LI-COR (Lincoln, NE, USA) C Di-Git blot scanner. Quantification was done using ImageJ.

Antibodies used were phospho-SMAD2 rabbit mAB 1:1000 in 5% BSA 4°C overnight, (#3108, Cell Signaling Technology, Danvers, MA, USA), goat anti-rabbit IgG (H + L)-HRP conjugate secondary antibody 1:3000 (Bio-Rad), and GAPDH rabbit mAB 1:1000, 1 hour RT (#2118, Cell Signaling Technology).

Immunohistochemistry

Cells were cultured for 14 days in 24-well black plates with flat coverslip bottom (ibidi). Fixation was done for 10 minutes at 37°C using Image-iT Fixative Solution (Thermo Fisher Scientific).

Table 3. Summary of *ADAMTSL2* (NM_014694.4, ENST00000393060.1, hg19) Variants in Families I–VIII

Family	Genomic position	cDNA	Protein	Exon	CADD[a]	MAF[b]	Inheritance
I	Chr9:g.136402593	c.157T>C	p.Trp53Arg	3	27.9	–	M
	Chr9:g.136433773	c.2137T>C	p.Cys713Arg	15	26.2	–	P
II	Chr9:g.136405809	c.502G>A	p.Gly168Ser	6	28.7	0.000004	P
	Chr9:g.136404920	c.337C>T	p.Arg113Cys	5	31.0	0.000006	M
III	Chr9:g.136438998	c.2626C>G	p.Arg876Gly	18	25.2	–	M/P
IV	Chr9:g.136402665	c.229C>T	p.Gln77*	3	43.0	0.000032	P
	Chr9:g.136412196	c.800G>T	p.Gly267Val	9	28.1	–	M
V	Chr9:g.136405803	c.496C>T	p.Arg166Cys	6	29.5	0.000004	P
	Chr9:g.136409627	c.718C>T	p.Arg240*	8	42.0	0.000004	M
VI	Chr9:g.136404921	c.338G>A	p.Arg113His[5,17]	5	32.0	0.000013	M
	Chr9:g.136419598	c.1061del	p.Gly354Alafs*7	10	26.0	–	P
VII	Chr9:g.136433518	c.1998C>G	p.Cys666Trp	14	19.6	–	P
	Chr9:g.136412340	c.939+5G>A	–	–	18.6	–	M
VIII	Chr9:g.136400041	c.-151+2T>C	–	–	22.3	0.000065	P
	Chr9:g.136433454	c.1934G>A	p.Arg645His[16]	14	26.3	–	M

Abbreviations: M = maternal; P = paternal; M/P = homozygous variant.
[a]Combined Annotation Dependent Depletion (CADD) score, model GRCh37-v1.6.
[b]Minor allele frequency (MAF) according to gnomAD v2.1.1.

After the fixation, cells were permeabilized for 10 minutes at room temperature using 1× eBioscience Permeabilization Buffer (Thermo Fisher Scientific). Cells were blocked in Serum-Free Protein Block (DAKO, Glostrup, Denmark) for 1 hour at room temperature. Primary antibody for FBN1 (HPA021057, Sigma-Aldrich, St. Louis, MO, USA) was diluted 1:200 in Ready-to-Use Antibody Diluent (DAKO), and cells were incubated overnight at 4°C. Incubation with secondary antibody (1:1000, anti-Rabbit Secondary Antibody, Alexa Fluor 488, Thermo Fisher Scientific) was done for 1 hour at RT. All washes were performed with 0.05% TBS-Tween (Thermo Fisher Scientific). Nuclei were stained by DAPI solution (Thermo Fisher Scientific), 1:1000 in TBS-Tween. Cells were mounted in ProLong Diamond Antifade Mountant (Thermo Fisher Scientific), and images were taken on LSM710 confocal microscope (Zeiss, Jena, Germany). Quantification was done using ImageJ software.

Statistical analysis

Statistical analysis was performed using GraphPad Prism 9 software (San Diego, CA, USA). Statistical significance was determined using Student's *t* test ($p < 0.05$). Data were presented as boxplots showing median, interquartile range, and minimum and maximum values.

Results

Clinical findings

The main clinical findings in Al-Gazali skeletal dysplasia patients included moderate intrauterine growth restriction (IUGR) detected in the second trimester, narrow thorax, short limbs and club feet, and dysmorphic features including flat facial profile, hypertelorism, depressed nasal bridge, protruding eyes, hypertrichosis, relative macrocephaly, low-set ears with abnormally thick helix, brachycephaly, stiff joints, and thick and tight skin (Fig. 1). Five of nine patients presented with internal abnormalities, including stenosis of the aorta and pulmonary artery, lung hypoplasia, right atrial, and bilateral ventricular dilatation (Table 1).

The main skeletal findings in our patients were generalized bone sclerosis, large anterior fontanelle, hypoplastic thorax with broad ribs, mild platyspondyly, absent or deficient ossification of pubic bones, short tubular bones, and severe brachydactyly (Fig. 2, Table 2).

Only two of the patients (5 and 8) have survived for more than 1 year. At the age of 12 months, patient 8 had significant hyperopia, possibly mild hearing loss, sleep apnea, narrow airway, pulmonary stenosis, and generalized stiffness. Radiological findings of patient 8 included severe brachydactyly, mild undermodeling of long bones of the arm (not shown), hypoplasia of ischial and pubic bones, and mild broadening of the ribs, but these features were milder compared with patient 5 (Fig. 2*B, C*). Patient 5 exhibited all radiological hallmarks of Al-Gazali skeletal dysplasia as well as unique fibular dysplasia and was not available for further follow-up of the clinical symptoms after the age of 14 months. Clinical and radiographic summaries for all patients are provided in Tables 1 and 2.

Genetic and molecular findings

The location and type of variants discovered in our patient cohort are shown in the schematic *ADAMTSL2* protein structure together with the previously reported variants associated with GPHYSD1 (Fig. 3*A*). All patients tested, except the fetus from family 3, were compound heterozygous for variants in *ADAMTSL2* (NM_014694.4, hg19) (Table 3). The patient sample in family 7 was not available for genetic investigation; however, analysis of parental samples identified a missense variant, c.1998C>G, p.(Cys666Trp), in the paternal sample and c.939+5G>A variant in the maternal sample. The maternal variant was predicted to affect splicing according to Alamut Visual Plus (v1.2, SOPHiA Genetics, St. Sulpice, Switzerland). Maternal RNA was not, however, available for further analysis. Two missense variants detected in our patient cohort, p.(Arg113His) in patient 3 and p.(Arg645His) in patient 8, were previously reported in patients with GPHYSD1.[5,16,17]

One of the variants identified in patient 8 (c.-151+2T>C) was paternally inherited and predicted to affect splicing (Alamut Visual Plus, v1.2, SOPHiA Genetics). Paternal blood sample from patient 8 was available for RNA analysis. It was hypothesized that the nucleotide change in the canonical splice site leads to no expression of the affected allele. Evaluation of the paternal WES data

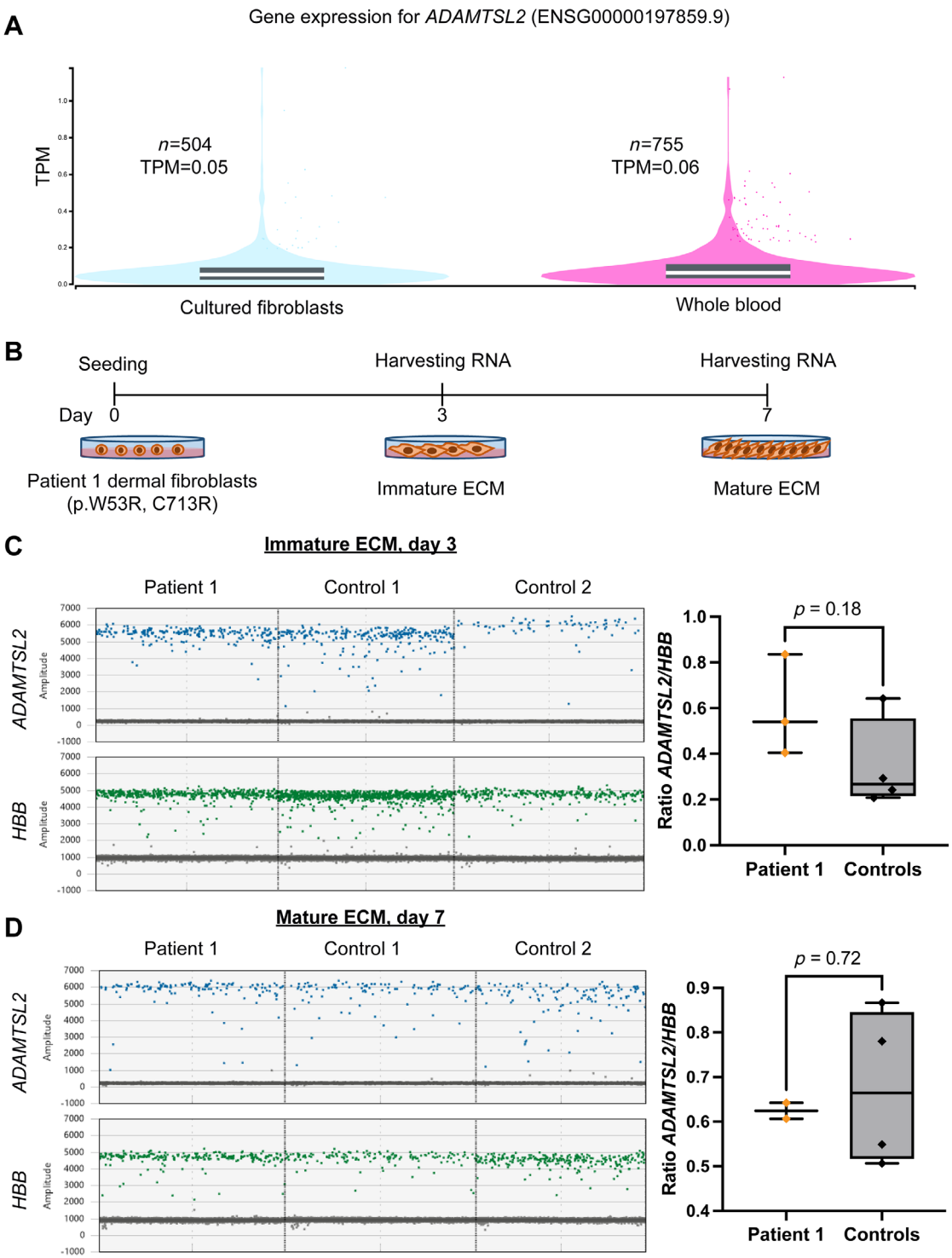

Fig. 4. *ADAMTSL2* gene expression analysis by ddPCR. (*A*) Graph generated from GTex database showing low expression of *ADAMTSL2* in most common clinically available tissues—cultured skin fibroblasts and whole blood. (*B*) Schematic representation of experimental conditions. RNA for ddPCR analysis was collected at two time points: day 3 (representing immature extracellular matrix [ECM] state) and day 7 (representing mature ECM state). (*C*) ddPCR data from dermal fibroblasts in immature ECM conditions. Left panel shows representative 1D plot of ddPCR data. Blue clusters indicate signals from the target gene *ADAMTSL2*. Green clusters indicate signals from the reference gene *HBB*. Right panel shows quantification of gene expression data, Student's *t* test, ±SEM. Two independent experiments with three biological and three technical replicates were performed. (*D*) ddPCR data from dermal fibroblasts cultured to reach mature ECM conditions. Left panel shows representative 1D plot of ddPCR data. Blue clusters indicate signals from the target gene *ADAMTSL2*, and green clusters from the reference gene *HBB*. Right panel shows quantification of gene expression data, Student's *t* test, ±SEM. Two independent experiments with three biological and three technical replicates were performed.

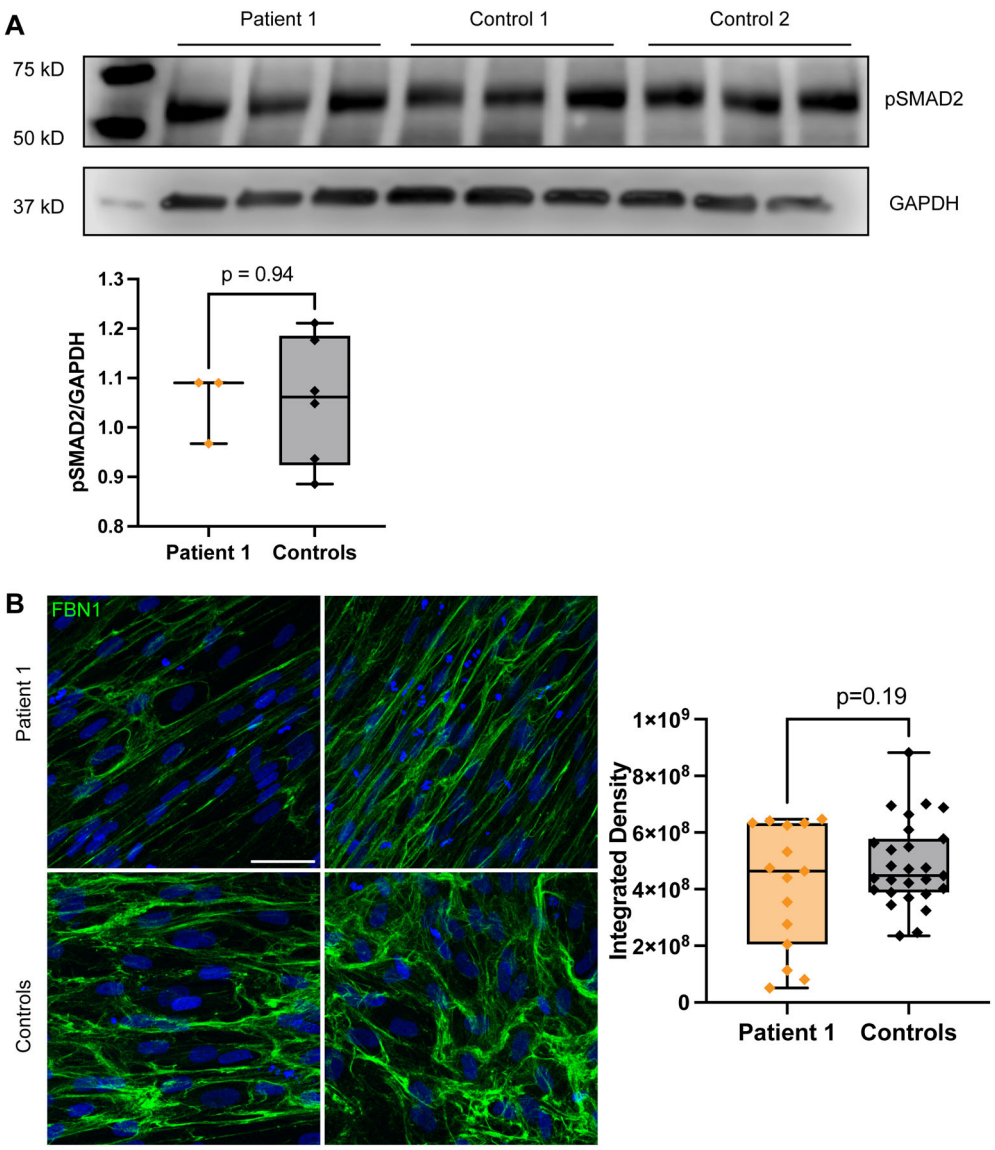

Fig. 5. Analysis of pSMAD2 expression and FBN1 microfibrillar network in primary dermal fibroblasts from Al-Gazali skeletal dysplasia patient and controls. (*A*) Western blot of pSMAD2 in primary dermal fibroblasts from patient 1 and two controls. Three biological replicates are shown for each sample. No statistically significant difference was observed between patient and control samples, Student's *t* test. (*B*) Immunofluorescence of fibrillin 1 (FBN1) in primary dermal fibroblasts from patient 1 and two controls. Note different patterns of denser and more stretched FBN1 microfibrillar network in patient (top) compared with controls (bottom). Additional images in Supplemental Fig. S1. No difference in signal intensity was observed as measured by mean integrated density across multiple images, Student's *t* test, scale bar = 50 μm.

identified four heterozygous single nucleotide variants (SNVs) in *ADAMTSL2*, which were targeted on cDNA level to confirm their hemizygous state. Figure 3*B* shows Sanger sequencing validation of one of the heterozygous variants (chr9:136421044 C > T, c.1641C>T, p.(His547=)), which appears as hemizygous on cDNA level and supports the pathogenicity of the c.-151+2T>C alteration.

ADAMTSL2 expression analysis by ddPCR

ADAMTSL2 has a very low expression in cultured dermal fibroblasts (median TPM = 0.0512, Fig. 4*A*) according to public databases (GTex, https://gtexportal.org/) and is poorly detectable using conventional qPCR methods. Thus, ddPCR was used to estimate the expression levels in primary dermal fibroblasts from patient 1, who was compound heterozygous for p.(Trp53Arg) and p.(Cys713Arg), and control samples. Gene expression was measured at two different time points to evaluate whether *ADAMTSL2* expression was dependent on different ECM conditions. RNA was collected at 95% confluency (3–4 days, immature ECM) and after 7 days in culture (mature ECM), as shown in Fig. 4*B*. Gene expression of *ADAMTSL2* at immature ECM conditions showed a minor increase in the patient 1 sample compared with controls but showed no statistical significance (Fig. 4*C*). At the mature ECM conditions, the patient 1 sample had comparable *ADAMTSL2* expression to

the control samples (Fig. 4D). Overall, similar *ADAMTSL2* expression levels were observed in patient and control samples regardless of the ECM conditions.

Analysis of pSMAD2 signaling and FBN1 microfibrillar network

Previous studies in primary cells of GPHYSD1 patients[5] and various mouse models suggest that the pathogenic mechanism of GPHYSD1 is an overactivation of TGFβ signaling pathway and/or affected microfibrillar network. In cultured dermal fibroblasts from patient 1 with Al-Gazali skeletal dysplasia, no differences in pSMAD2 expression were observed compared with controls (Fig. 5A). In addition, the microfibrillar network organization was explored by imaging FBN1 microfibrils (Fig. 5B and Supplemental Fig. S1). FBN1 had comparable signal intensity between patient 1 and controls. However, distribution pattern of FBN1 microfibrils in patient 1 showed more stretched and denser FBN1 microfibrils compared with controls. These differences were more evident in the lower-magnification images (Supplemental Fig. S1).

Discussion

In this study, we summarize clinical and genetic findings of nine individuals with Al-Gazali skeletal dysplasia, two of whom have previously been described by Grigelioniene and colleagues.[2] We report for the first time that biallelic variants in the *ADAMTSL2* gene cause skeletal dysplasia Al-Gazali type.

ADAMTSL2 is a disease-causing gene in geleophysic dysplasia type I (GPHYSD1), the severe forms of which show early lethality and a similar clinical and radiographic presentation to Al-Gazali skeletal dysplasia.[5,16,18] In addition to *ADAMTSL2*, *FBN1* and *LTBP3* genes are also associated with GPHYSD2 and GPHYSD3, respectively. Disease-causing variants are spread across the *ADAMTSL2* protein (Fig. 3A), whereas variants in *FBN1* are localized in one specific TB5 domain. Five individuals with *LTBP3*-associated GPHYSD and varying degrees of disease severity have also been described.[19] The evident genetic heterogeneity in geleophysic dysplasia and the variation of phenotype severity in affected individuals indicate the broad disease spectrum.

Herein, we suggest that Al-Gazali skeletal dysplasia is the most severe form of *ADAMTSL2*-related conditions and that there is a phenotypic continuum in geleophysic and Al-Gazali skeletal dysplasias. The distinction between two conditions can be made on the basis of radiological features. The hallmarks, such as generalized osteosclerosis, severe brachydactyly and a very short first metacarpal, undermodeling of the long bones, broad ribs, and mild misalignment of the elbow, are unique for Al-Gazali skeletal dysplasia, and not commonly found in GPHYSD1 (Supplemental Table 2). However, it is likely that the milder phenotype of Al-Gazali skeletal dysplasia, such as in patient 8 in this study, overlaps with the most severe features of geleophysic dysplasia.[18]

The pseudogene region of the *ADAMTSL2* gene is poorly covered in the major genomic databases using GRCh37/hg19 genome build (gnomAD v2.1.1), creating read alignment challenges when using exome or genome sequencing for clinical diagnostics.[20] In addition, *ADAMTSL2* has been identified as one of the eight genes where discrepant variant calls are influenced by the choice of reference assembly (GRCh37 versus GRCh38).[21] *ADAMTSL2* coverage is significantly improved in the GRCh38 genome build, as found in gnomAD v.3.1.2 (Fig. 6), indicating that the read alignment challenge is caused by selection of reference genome. GRCh37 is still widely used in whole genome or exome sequencing analysis in the clinical diagnostics

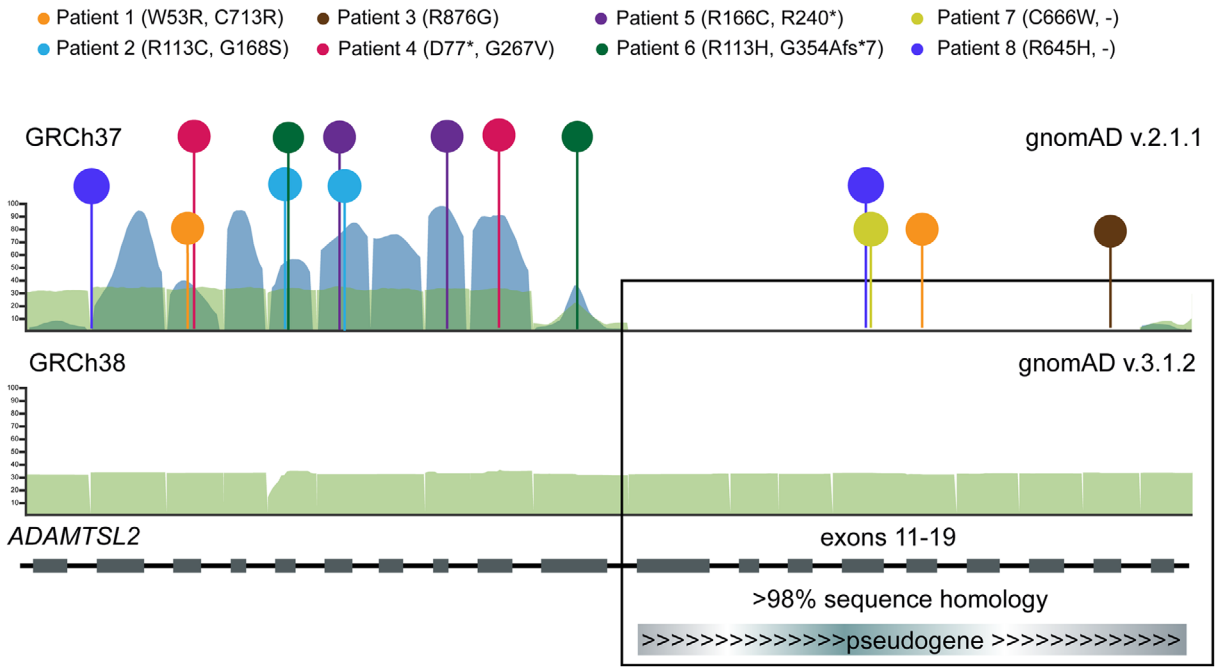

Fig. 6. Coverage discrepancies in *ADAMTSL2* sequence. Comparison of *ADAMTSL2* coverage in different genome assemblies in gnomAD database (https://gnomad.broadinstitute.org/). Exons 11–19 are affected by segmental duplication and share >98% homology with a pseudogene region assembly (rectangular selection). The region is poorly covered in GRCh37 assembly. Variants detected in this study are shown in different colors.

setting. If diagnosis of Al-Gazali or GPHYSD1 is suspected based on radiographic findings but only single candidate variant is detected in *ADAMTSL2*, one should manually inspect the poorly mapped reads for potential disease-causing variants. Alternatively, more advanced sequencing methods, such as long-read sequencing, would enable more accurate variant calling. The identification of disease variants that are located in the pseudogene region of *ADAMTSL2* highlights the importance of meticulous phenotyping and selection of the appropriate genetic analysis method, including the analysis of non-coding exon of the *ADAMTSL2* gene.

The direct analysis of variant impact on *ADAMTSL2* gene expression in patient samples is complicated because of low *ADAMTSL2* mRNA levels in commonly clinically available tissues. In our study, we show that it is possible to detect *ADAMTSL2* expression in primary human dermal fibroblasts using ultrasensitive detection method, ddPCR. Even though significant differences in *ADAMTSL2* expression between patient and control samples were not observed, it is possible that the slight change of expression levels in different culturing conditions (immature and mature ECM) indicates the importance of *ADAMTSL2* in ECM assembly and function. Our observation is limited by the very small sample size, and further studies are needed to confirm these findings in primary human cells.

Multiple insights into the role of *ADAMTSL2* at organism and tissue level have been generated from in vivo studies. *Adamtsl2*$^{-/-}$ mice die soon after birth because of severe lung dysfunction and bronchial epithelial dysplasia, accompanied by accumulation of fibrillin microfibrils in the bronchial epithelia.[22] The described phenotype in mice resembles that of GPHYSD and Al-Gazali skeletal dysplasia patients suffering from narrowing of the trachea and recurrent respiratory infections. Downregulation of *Adamtsl2* expression in bronchi after E17.5 suggests that *Adamtsl2* could have a crucial role during early development, thus possibly explaining early lethality in affected individuals. The skeletal phenotype of *Adamtsl2* KO mice was analyzed in more detail in another study and showed significant shortening of forelimbs and hindlimbs, shorter long bones, slight deformation of vertebral bodies, and shortened calvaria.[23] However, the early perinatal lethality of *Adamtsl2* KO mice did not permit examination of the postnatal skeletal phenotype in more detail. Nonetheless, on the cellular level, the formation of chondrocyte columns in the long bones was significantly affected in conditional Adamtsl2-Col2a1Cre mice, recapitulating the skeletal dysplasia phenotype in GPHYSD1.[23] A similar observation was made in the Prx1-Cre conditional *Adamtsl2* knockout model, where *Adamtsl2*-Prx mice had shorter forelimb and distal bones and wider diaphyseal and metaphyseal regions.[24] Contrasting observations in regard to growth plate phenotype were noted in both studies. Whereas *Adamtsl2*-Prx mice had normal growth plate morphology, the Col2a-mediated chondrocyte-specific deletion led to growth plate abnormalities.[23,24] Moreover, *Adamtsl2*-Prx mice exhibited shorter and fibrotic Achilles tendons, with an excess of FBN1 microfibrils. The tendon phenotype of *Adamtsl2* mice has further been studied using the tendon-specific *Adamtsl2* deletion model (*Adamtsl2*-Scx). *Adamtsl2*-Scx mice also had shorter limbs but an overall milder bone phenotype compared with *Adamtsl2*-Prx mice.[22,24]

The biological mechanism of how pathogenic variants in *ADAMTSL2* lead to skeletal dysplasia are thought to be through abnormalities in TGFβ signaling and/or affected microfibrillar network composition and morphology.[3,5] It is not entirely clear if the overactivation of the TGFβ signaling pathway is a secondary consequence of affected ECM organization. We did not observe differences in TGFβ signaling as measured by pSMAD2 levels. This is consistent with findings in another type of acromelic dysplasia, Weill-Marchesani syndrome, where no changes in TGFβ signaling were noted in primary human fibroblasts.[4] Moreover, the overactivation of TGFβ signaling in bronchial tissue in mice was observed only during the embryonic period and was not rescued by TGFβ antibody treatment.[22] The molecular and in vivo data provide evidence that *ADAMTSL2* binds to ECM components FBN1, FBN2, and LTBP1, and is important for proper ECM function.[5,22,24] Different distribution pattern of FBN1 microfibrils was found in cultured cells from patient 1 with Al-Gazali skeletal dysplasia. Previous studies in mice show evident abnormalities of various ECM components upon genetic manipulation of *Adamtsl2* in connective tissues.[22–24] However, more extensive studies of ECM in human samples are needed to confirm the pathogenic effects of *ADAMTSL2* variants on ECM assembly and function. In a review by Stanley and colleagues, a conceptual model was proposed to decipher the interaction between several ECM proteins within the acromelic dysplasia complex, where FBN1 microfibrils serve as a crucial ECM hub to bring ADAMTS(L) and LTBP proteins and control TGFβ and BMP signaling pathways.[3] Furthermore, Steinle and colleagues described five unrelated individuals with dermatosparaxic Ehlers-Danlos syndrome (dEDS) presenting with generalized joint hypermobility and fragility of the connective tissue caused by an autosomal dominant variant in *ADAMTSL2* (c.1261G>A, p.(Gly421Ser)).[25] The contrasting clinical features of connective tissue laxity in dEDS versus tissue rigidity in GPHYSD1 and Al-Gazali skeletal dysplasias suggests the possible gain-of-function effect of the p.(Gly421Ser) variant and thus further expands the spectrum of ADAMTSL2-related disorders.

In conclusion, this study adds Al-Gazali skeletal dysplasia to the clinical and genetic spectrum of ADAMTSL2-related disorders and indicates the need for further molecular studies to understand the impact of different mutations on phenotypic variability and to explain the summative interaction of important molecular players within the ECM microenvironment.

Acknowledgments

We thank all the patients and their family members for participating in the study. We acknowledge support from SciLifeLab, Clinical Genomics, National Genomics Infrastructure (NGI), Broad Institute of MIT and Harvard Center for Mendelian Genomics (Broad CMG), and Uppmax for sequencing and computational infrastructure. We thank Jesper Eisfeldt and Daniel Nilsson for valuable input regarding bioinformatic analysis. We thank Prof Jürgen W Spranger for diagnostic insights. We acknowledge methodological support from Jakob Schuy and Gustaw Eriksson.

Financial support was provided by grants from Karolinska Institutet grant for doctoral education (DB), Stiftelsen Sällsyntafonden (DB, FT), Stiftelsen Sällskapet Barnavård (AH), Stiftelsen Promobilia (GG), Stiftelsen Frimurare (AN, GG), Swedish Research Council and the Region Stockholm (AN, GG), Bertil Hållsten Research Foundation (AN), and Karolinska Institutet (AH, FT, GG).

Patient six was a part of the NHMRC-funded Genomic Autopsy Study (APP1123341) supported by the Australian Genomic Health Alliance NHMRC Targeted Call for Research into Preparing

Australia for the Genomics Revolution in Healthcare (GNT1113531) to HSS and CPB. Sequencing for patient six was provided by the Broad Institute of MIT and Harvard Center for Mendelian Genomics (Broad CMG), which was funded by the National Human Genome Research Institute, the National Eye Institute, and the National Heart, Lung and Blood Institute grant UM1 HG008900 to Daniel MacArthur and Heidi Rehm.

Some of the authors (AN, AL, GG) of this publication are members of the European Reference Network on Rare Congenital Malformations and Rare Intellectual Disability ERN-ITHACA (EU Framework Partnership Agreement ID: 3HP-HP-FPA ERN-01-2016/739516).

The study was approved by the Regional Ethical Review Board for Karolinska University Hospital (protocol numbers 2014/983-31/1, 2014/430-31, 2012/2106-31/4, 2018/2207-32, and 2021-05360), Human Ethics Committee of the Melbourne Health Human Research Ethics Committee as part of the Australian Genomics Health Alliance (protocol HREC/16/MH/251), Ethics Committee of Saitama Children's Medical Center (protocol number 2015-04-004). Informed consent was obtained from the parents or legal guardians of each patient.

Author Contributions

Dominyka Batkovskyte: Conceptualization; formal analysis; investigation; methodology; validation; visualization; writing – original draft; writing – review and editing. **Fiona McKenzie:** Conceptualization; resources; writing – review and editing. **Fulya Taylan:** Conceptualization; data curation; formal analysis; methodology; writing – review and editing. **Pelin Ozlem Simsek-Kiper:** Data curation; investigation; validation; writing – review and editing. **Sarah M. Nikkel:** Data curation; writing – review and editing. **Hirofumi Ohashi:** Data curation; investigation. **Roger E. Stevenson:** Formal analysis; investigation; writing – review and editing. **Thuong Ha:** Data curation; formal analysis; investigation; writing – review and editing. **Denise P. Cavalcanti:** Data curation; writing – review and editing. **Hiroyuki Miyahara:** Data curation; investigation. **Steven A. Skinner:** Investigation; writing – review and editing. **Miguel A. Aguirre:** Data curation. **Zühal Akçören:** Data curation; investigation; writing – review and editing. **Gulen Eda Utine:** Data curation; investigation; validation; writing – review and editing. **Tillie Chiu:** Resources. **Kenji Shimizu:** Data curation; investigation. **Anna Hammarsjö:** Data curation; funding acquisition; project administration; writing – review and editing. **Koray Boduroglu:** Investigation; data curation; validation; writing – review and editing. **Hannah W. Moore:** Investigation; writing – review and editing. **Raymond J. Louie:** Formal analysis; investigation; writing – review and editing. **Peer Arts:** Formal analysis; writing – review and editing. **Allie N. Merrihew:** Investigation; writing – review and editing. **Milena Babic:** Project administration; writing – review and editing. **Matilda R. Jackson:** Project administration; writing – review and editing. **Nikos Papadogiannakis:** Visualization; data curation. **Anna Lindstrand:** Data curation; writing – review and editing; resources. **Ann Nordgren:** Data curation; resources. **Christopher P. Barnett:** Conceptualization; funding acquisition; supervision; writing – review and editing. **Hamish S. Scott:** Conceptualization; funding acquisition; supervision; writing – review and editing. **Andrei S. Chagin:** Methodology; supervision. **Gen Nishimura:** Conceptualization; data curation; formal analysis; writing – review and editing. **Giedre Grigelioniene:** Conceptualization; data curation; formal analysis; project administration; supervision; resources; funding acquisition; writing – original draft; writing – review and editing.

Conflicts of Interest

AL has received honoraria from Illumina. The funders had no role in the design of the study, in the collection, analyses, or interpretation of data, in the writing of the manuscript, or in the decision to interpret and publish the results.

Peer Review

The peer review history for this article is available at https://www.webofscience.com/api/gateway/wos/peer-review/10.1002/jbmr.4799.

Data Availability Statement

All identified variants are submitted to ClinVar database, accession numbers: SCV002583305-SCV002583318. Complete data are not publicly available due to privacy and ethical restrictions. Other data supporting the findings of this study are available from the corresponding author upon reasonable request.

References

1. Al-Gazali L, Devadas K, Hall CM. A new lethal neonatal short limb dwarfism. Clin Dysmorphol. 1996;5:154–164.
2. Grigelioniene G, Papadogiannakis N, Conner P, Geiberger S, Nishikawa M, Nakayama M. Extending the phenotype of lethal skeletal dysplasia type al Gazali. Am J Med Genet A. 2011;155A(6):1404–1408.
3. Stanley S, Balic Z, Hubmacher D. Acromelic dysplasias: how rare musculoskeletal disorders reveal biological functions of extracellular matrix proteins. Ann N Y Acad Sci. 2020;1490:57–76.
4. Arnaud P, Mougin Z, Boileau C, Le Goff C. Cooperative mechanism of ADAMTS/ADAMTSL and Fibrillin-1 in the Marfan syndrome and acromelic dysplasias. Front Genet. 2021;12:734718.
5. Le Goff C, Morice-Picard F, Dagoneau N, et al. ADAMTSL2 mutations in geleophysic dysplasia demonstrate a role for ADAMTS-like proteins in TGF-beta bioavailability regulation. Nat Genet. 2008;40(9):1119–1123.
6. Marzin P, Thierry B, Dancasius A, et al. Geleophysic and acromicric dysplasias: natural history, genotype-phenotype correlations, and management guidelines from 38 cases. Genet Med. 2021;23(2):331–340.
7. Allali S, Le Goff C, Pressac-Diebold I, et al. Molecular screening of ADAMTSL2 gene in 33 patients reveals the genetic heterogeneity of geleophysic dysplasia. J Med Genet. 2011;48(6):417–421.
8. Unger S, Ferreira CR, Mortier GR, et al. Nosology of genetic skeletal disorders: 2023 revision. Am J Med Genet A. 2023. [published online ahead of print, 2023 Feb 13].
9. Rypdal KB, Erusappan PM, Melleby AO, et al. The extracellular matrix glycoprotein ADAMTSL2 is increased in heart failure and inhibits TGFbeta signalling in cardiac fibroblasts. Sci Rep. 2021;11(1):19757.
10. Stranneheim H, Lagerstedt-Robinson K, Magnusson M, et al. Integration of whole genome sequencing into a healthcare setting: high diagnostic rates across multiple clinical entities in 3219 rare disease patients. Genome Med. 2021;13(1):40.
11. Rentzsch P, Witten D, Cooper GM, Shendure J, Kircher M. CADD: predicting the deleteriousness of variants throughout the human genome. Nucleic Acids Res. 2019;47(D1):D886–d94.
12. McLaren W, Gil L, Hunt SE, et al. The Ensembl variant effect predictor. Genome Biol. 2016;17(1):122.

13. Lek M, Karczewski KJ, Minikel EV, et al. Analysis of protein-coding genetic variation in 60,706 humans. Nature. 2016;536(7616): 285–291.
14. Voigt M, Fusch C, Olbertz D, et al. Analysis of the neonatal collective in the Federal Republic of Germany 12th report: presentation of detailed percentiles for the body measurement of newborns. Geburtshilfe Frauenheilkd. 2006;66:956–970.
15. World Health Organization. Child growth standards. Geneva, Switzerland: WHO; 2005.
16. Porayette P, Fruitman D, Lauzon JL, et al. Novel mutations in geleophysic dysplasia type 1. Pediatr Dev Pathol. 2014;17(3): 209–216.
17. Elhoury ME, Faqeih E, Almoukirish AS, Galal MO. Cardiac involvement in geleophysic dysplasia in three siblings of a Saudi family. Cardiol Young. 2015;25(1):81–86.
18. Panagopoulos P, Fryssira H, Koutras I, et al. Geleophysic dysplasia: a patient with a severe form of the disorder. J Obstet Gynaecol. 2005; 25(8):818–820.
19. McInerney-Leo AM, Le Goff C, Leo PJ, et al. Mutations in LTBP3 cause acromicric dysplasia and geleophysic dysplasia. J Med Genet. 2016; 53(7):457–464.
20. Karczewski KJ, Francioli LC, Tiao G, et al. The mutational constraint spectrum quantified from variation in 141,456 humans. Nature. 2020;581(7809):434–443.
21. Li H, Dawood M, Khayat MM, et al. Exome variant discrepancies due to reference-genome differences. Am J Hum Genet. 2021;108(7): 1239–1250.
22. Hubmacher D, Wang LW, Mecham RP, Reinhardt DP, Apte SS. Adamtsl2 deletion results in bronchial fibrillin microfibril accumulation and bronchial epithelial dysplasia—a novel mouse model providing insights into geleophysic dysplasia. Dis Model Mech. 2015; 8(5):487–499.
23. Delhon L, Mahaut C, Goudin N, et al. Impairment of chondrogenesis and microfibrillar network in Adamtsl2 deficiency. FASEB J. 2019; 33(2):2707–2718.
24. Hubmacher D, Taye N, Balic Z, et al. Limb- and tendon-specific Adamtsl2 deletion identifies a role for ADAMTSL2 in tendon growth in a mouse model for geleophysic dysplasia. Matrix Biol. 2019;82: 38–53.
25. Steinle J, Hossain WA, Lovell S, Veatch OJ, Butler MG. ADAMTSL2 gene variant in patients with features of autosomal dominant connective tissue disorders. Am J Med Genet A. 2021;185(3):743–752.